# Absence of a pressure-induced structural phase transition in $Ti_3Al$ up to 25 GPa

N. A. Dubrovinskaia,[1] M. Vennström,[2] I. A. Abrikosov,[3] R. Ahuja,[3] P. Ravindran,[4] Y. Andersson,[2] O. Eriksson,[3] V. Dmitriev,[5] and L. S. Dubrovinsky[1]

[1]*Department of Earth Sciences, Uppsala University, S-75236 Uppsala, Sweden*

[2]*Department of Inorganic Chemistry, Uppsala University, S-75123, Uppsala, Sweden*

[3]*Condensed Matter Theory Group, Physics Department, Uppsala University, S-75121 Uppsala, Sweden*

[4]*Department of Chemistry, University of Oslo, Blindern, N-0315 Oslo, Norway*

[5]*European Synchrotron Radiation Facilities (ESRF), BP 220, F-38043 Grenoble Cedex, France*

(Received 19 September 2000; published 18 December 2000)

Experimental high-pressure studies of titanium aluminide ($Ti_3Al$) have been carried out under quasihydrostatic and nonhydrostatic conditions up to a pressure of 25 GPa using an *in situ* powder x-ray diffraction technique. The experiments were complemented by first-principles total energy calculations. The experimental equation of state for three samples with different compositions was fitted using the Birch-Murnaghan equation. The obtained parameters agree very well with theoretical results. In the studied pressure range neither experiment nor theory observed any pressure-induced structural phase transition. In particular, the phase transition from the $DO_{19}$ ($Ni_3Sn$ type) structure of $Ti_3Al$ to $DO_{24}$ ($Ni_3Ti$ type) structure, reported earlier by Sahu *et al.* [Phys. Rev. Lett. **78**, 1054 (1997)] is not confirmed in our study. Possible reasons for the discrepancy are analyzed.

DOI: 10.1103/PhysRevB.63.024106 PACS number(s): 62.50.+p, 64.70.Kb

Titanium and its alloys are traditional engineering materials that possess an extraordinary combination of properties.[1] They are commonly utilized in aerospace, space vehicles, and in the petroleum and chemical industries. In particular, the phase $Ti_3Al$ ($Ni_3Sn$-type structure) exhibits low density and good high-temperature strength and was therefore chosen for development of aircraft engines materials.[2] However, one of the main technological problems with $Ti_3Al$ is to increase the room-temperature ductility of this ($Ni_3Sn$-type) brittle phase. In practice, the ductility is increased by alloying $Ti_3Al$ with 8–18 % Nb (other possible alloying elements are Mo, V, Ta, and Ni), but other more efficient ways to increase the ductility are being pursued. One avenue that is being pursued quite generally in order to improve on the ductility is to increase the number of active slip planes to satisfy the von Mises criterion. Crystal structure plays very important role in determining the ductility. For this reason the goal has become to transform the material of interest into cubic crystal structure, since often these structures display many active slip planes. It is for this reason a structural investigation of $Ti_3Al$ becomes important, since if the mechanisms that are pertinent for the structural stability is understood one may find ways to synthesize this material in a cubic (and hopefully more ductile) phase.

Recently, a high pressure investigation of $Ti_3Al$ was made by Sahu *et al.*[3] in order to study its structural phase stability behavior. These authors have reported a structural phase transition from the $DO_{19}$ ($Ni_3Sn$-type) to the $DO_{24}$ ($Ni_3Ti$-type) structure in the pressure range of 10–15 GPa. In a subsequent paper by Rajagopalan *et al.*[4] this finding was seemingly confirmed by theoretical calculations. However, the high pressure study in Ref. 3 was carried out on one single sample, and the interpretation of the results was not unambiguous as well as the calculations reported in Ref. 4 were carried out within the so-called atomic sphere approximation (ASA) which sometimes fails to resolve small structural energy differences. Therefore, we decided to conduct a series of experiments on a number of samples with compositions covering the whole homogeneity range (22–38 at. % Al) of $Ti_3Al$, and to complement them by first-principles total energy calculations of the competing phases of $Ti_3Al$ using the ASA, as well as much more accurate full-potential method.

Three samples were prepared by arc melting appropriate amounts of titanium rod (99.98% Materials research S.A.) and aluminum ingot (99.999 % Granges S.M.) in an arc furnace in a pure argon atmosphere. The samples were powdered by milling and then homogenized in vacuum at 900 °C for 5 h. For the compressibility study we used the DXR-GMW diamond anvil cell (DAC) (Diacell Products, UK) described elsewhere.[5] Pt, Ag, Cu, and NaCl served as internal standards for pressure calibration and the pressures were determined with accuracies better than 1 GPa by using known equations of state.[6] For every composition of $Ti_3Al$, 33.3, 28.4, and 24 at. % Al, a series of experiments with various pressure calibrants and with, as well as without, methanol-ethanol-water (MEW) mixture as a pressure-transmitting medium were conducted.[7] The MEW provides hydrostatic conditions up to 15 GPa.[8] In experiments with NaCl as a pressure calibrant and MEW mixture as a pressure medium, the unit cell parameter of NaCl was determined using separately three reflections (111), (200), and (220). All the three values agree with each other within 0.0005 Å at pressures up to 19 GPa. This means that stresses are negligibly small at these conditions.[9]

Theoretical calculations have been carried out in the framework of the density functional theory employing the generalized gradient approximation (GGA) (Ref. 10) for the exchange-correlation potential and energy. We employed the linear-muffin-tin-orbital (LMTO) method of Andersen.[11] The effective one-electron potential was treated within the ASA,[11] as well as without any shape approximation by

 

TABLE I. Lattice parameters $a$ and $c$ (in Å), unit cell volumes $V$ (in Å$^3$), bulk moduli $K_{300,1}$ (in GPa) and their pressure derivatives $K'_{300,1}$ for $Ti_3Al$ obtained by different experimental and theoretical techniques.

| Sample | $a$ | $c$ | $V$ | $K_{300,1}$ | $K'_{300,1}$ |
|---|---|---|---|---|---|
| $Ti_{76.0}Al_{24.0}$ [a] | 5.8083(7) | 4.6563(5) | 136.04(4) | 133(8) | 2.6(8) |
| $Ti_{76.0}Al_{24.0}$ [b] | 5.79 | 4.69 | 136.4 | 124 | 3.4 |
| $Ti_{71.6}Al_{28.4}$ [a] | 5.7829(4) | 4.6388(4) | 134.35(2) | 131(8) | 3.6(1.4) |
| $Ti_{71.6}Al_{28.4}$ [b] | 5.78 | 4.68 | 135.5 | 123 | 3.5 |
| $Ti_{66.7}Al_{33.3}$ [a] | 5.7763(4) | 4.6348(4) | 133.92(2) | 125(6) | 4.4(9) |
| $Ti_{66.7}Al_{33.3}$ [b] | 5.77 | 4.67 | 134.7 | 122 | 3.5 |
| $Ti_3Al$ [c] | 5.775 | 4.638 | 133.96 | | |
| $Ti_3Al$ [d] | 5.77 | 4.62 | 133.21 | | |
| $Ti_{2.88}Al_{1.12}$ [e] | 5.780 | 4.647 | 134.45 | | |
| $Ti_3Al$ [f] | 5.818 | 4.689 | 137.45 | 106.7(5.8) | |
| $Ti_3Al$ [g] | | | 127.8 | 128.87 | |

[a]This work, experiment.
[b]This work, theory. Presented results were obtained by means of LMTO-ASA-CPA technique, and $c/a$ ratio was optimized for ordered $Ti_3Al$ by means of FP-LMTO method, and then fixed.
[c]Experiment, Ref. 16.
[d]Experiment, Ref. 17.
[e]Experiment, Ref. 18.
[f]Experiment, Ref. 3.
[g]Theory, Ref. 4. Unit cell volume was extracted from Fig. 4 of Ref. 4 using experimental volume of Ref. 3.

means of an accurate full-potential (FP) technique.[12] The former approach allows us to take into account the effect of disorder within the multisublattice generalization of the coherent potential approximation (CPA),[13] and to calculate accurate total energy differences between *different atomic arrangements on the same underlying crystal lattice*. In contrast to the ASA (also used in Ref. 4), the FP method is particularly suitable for resolving small *structural* energy differences in ordered intermetallic compounds and therefore it is widely used for studies of structural phase transitions.[14] In particular, in our FP-LMTO calculations, we have used 1000 $k$ points in the irreducible part of the Brillouin zone of the DO19 and DO24 structures, and we have converged our total energies with respect to $k$ points and basis set up to 0.05 mRy. Note that the present full-potential approach is known to give an accuracy of the total energy within $\mu$e V range.[15]

To illustrate the reliability of the combined experimental and theoretical approach to the problem, the determined unit cell parameters and molar volumes are shown in Table I. For a comparison, parameters available in the literature are also listed.[16–18] Both the $a$ and $c$ unit cell parameters decrease with increasing Al content, which is in correspondence with smaller radius of Al than that of Ti. The good agreement between the theory and the experiment is typical for modern *ab initio* calculations.

The dependence between the unit cell volume and the pressure, both from experiments and theory, is shown in Fig. 1(a) for all three samples. Again, the agreement between theory and experiment is found to be quite satisfactory. The $P$-$V$ experimental data was fitted to the Birch-Murnaghan

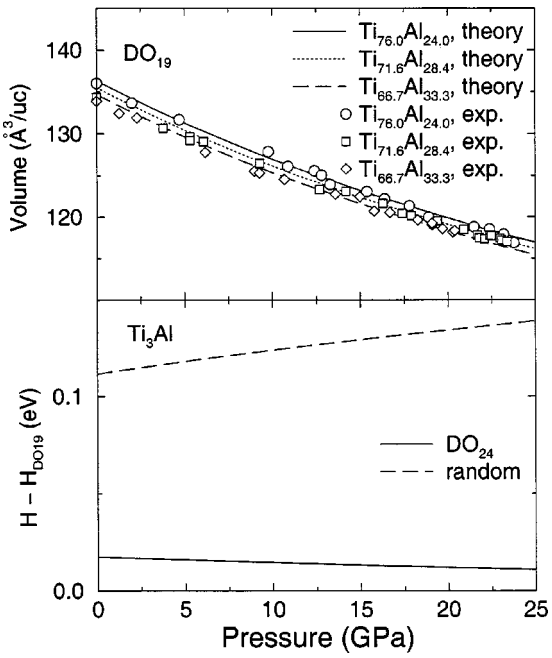


FIG. 1. (a) Experimental (circles, squares, and diamonds) and theoretical (lines) dependences between the unit cell volume and pressure for the $Ti_3Al$ alloys with 24 at. % Al (solid line, circles), 28.4 at. % Al (dotted line, squares), and 33.3 at. % Al (dashed line, diamonds). Theoretical results are obtained by the LMTO-ASA-CPA method. The FP-LMTO PV diagram for ordered $Ti_3Al$ is not shown, but is in very good agreement with those for off-stoichiometric alloys presented in this figure. (b) Calculated pressure dependence of the enthalpy $H$ for stoichiometric $Ti_3Al$ with $DO_{24}$ structure (solid line, FP-LMTO calculations) and disordered hcp $Ti_3Al$ alloy (dashed line, LMTO-ASA-CPA calculations) relative to the enthalpy of ordered $DO_{19}$ $Ti_3Al$.

equation of state.[19] The volume of the unit cell at zero pressure and room temperature $V_{300,0}$ for all three phases was found with high accuracy, and therefore a fixed $V_{300,0}$ was used in the fitting procedure. The values of the bulk modulus $K_{300,1}$ and its pressure derivative $K'_{300,1}$ are also presented in Table I. There is a correlation between the values of $K_{300,1}$ and $K'_{300,1}$ and the Al content. The bulk modulus decreases and its pressure derivative increases with increasing Al concentration. Similar trends are also seen in the theoretical results. Note that the values of $K_{300,1}$ for all three alloys are significantly higher than the value reported by Sahu *et al.*[3] [106.7(5.8) GPa, Table I].

The central question of the present study is to investigate possible pressure induced structural phase transition in $Ti_3Al$ at pressures up to 25 GPa. The experiment with the 33.3 at. % Al sample was conducted under the same conditions as described in the paper by Sahu *et al.*[3] A pure silver powder was used as pressure calibration standard and MEW was used as pressure-transmitting medium.[7] Diffraction patterns were registered upon compression (up to 21 GPa) and decompression, and the results are shown in Fig. 2 [curves denoted (a), (c), and (e)]. The only change in the diffraction patterns, except shifts of reflections to lower $d$ spacings, was disappearances of the (101), (110), and (211) superlattice

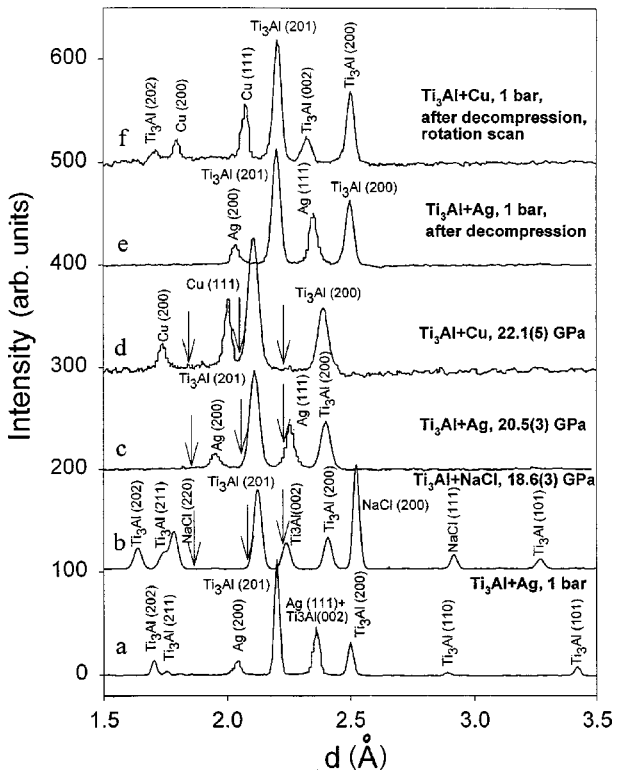


FIG. 2. The diffraction patterns of the various $Ti_3Al$ alloys at different pressures. (a) $Ti_3Al$ with 33.3 at. % Al (Ag was used as an internal standard for pressure calibration), $P=1$ bar; (b) $Ti_3Al$ with 24 at. % Al (NaCl was used as a pressure calibration standard), $P=18.6(3)$ GPa. This diffraction pattern was collected at ESRF. (c) $Ti_3Al$ with 33.3 at. % Al at $P=20.5(3)$ GPa; (d) $Ti_3Al$ alloy with 24 at. % Al (Cu was used as an internal standard for pressure calibration), $P=22.1(5)$ GPa; (e) $Ti_3Al$ with 33.3 at. % Al after decompression; (f) $Ti_3Al$ alloy with 24 at. % Al (Cu was used as an internal standard for pressure calibration) after decompression-rotation scan. The estimated positions of the most intense reflections from the $Ni_3Ti$ type structure ($DO_{24}$) are marked with arrows.

reflections, as well as the (002) and (202) reflections of $Ti_3Al$ at elevated pressures (above 20 GPa).

For $Ti_3Al$ with 28.4 at. % Al we conducted two experiments, with and without pressure-transmitting medium, using a piece of pure Pt wire (10 $\mu$m in diameter) as a pressure calibrant. We reached 25 GPa and registered *in situ* x-ray diffractograms both on compression and decompression. No additional changes in the diffraction patterns compared to the 33.3 at. % Al alloy were found in the experiments both under nonhydrostatic and hydrostatic conditions. Note that experiments conducted under nonhydrostatic conditions, may induce a phase transition at a different pressure compared to hydrostatic experiments. As a matter of fact non-hydrostatic pressures may even result in phase transitions to metastable phases.

For the specimen with the lowest Al content (24 at. %), three experiments were performed. One with Pt powder (particle size 2 $\mu$m), one with a copper wire and one with NaCl as the pressure calibration standards. The diffraction pattern shown in Fig. 2 [curve denoted (d)] was recorded at a pressure of 22.1(5) GPa. Cu was chosen as a standard especially to ''clean'' the area where the new reflections were observed by Sahu and co-authors.[3] Moreover, the curve denoted as (b) in Fig. 2 shows the x-ray diffraction pattern of $Ti_{76}Al_{24}$ collected at the European Synchrotron Radiation Facilities (ESRF). Here NaCl was used as a pressure calibration standard. At pressure 18.63 GPa the difraction pattern contains all six reflections of the $DO_{19}$ structure of $Ti_3Al$. Figure 2 shows that no extra reflections appear up to 25 GPa, but the superlattice reflections (101), (110), and (211), as well as the (002) and (202) reflections disappear at pressures above 20 GPa. According to earlier study by Sahu *et al.*[3] a complete phase transition of $Ti_3Al$ with the $Ni_3Sn$-type ($DO_{19}$) structure to the $Ni_3Ti$-type ($DO_{24}$) structure should occur between 10–15 GPa. The estimated positions of the reflections from the $Ni_3Ti$-type structure are marked with arrows in Fig. 2. Thus, no evidence of a structural phase transition of $Ti_3Al$ was found in the present experiments, and the absence of the $DO_{24}$ phase was clearly established by the absence of the most intensive characteristic reflections of this phase in the pressure range up to 25 GPa.

To investigate this finding further, we have carried out total energy electronic structure calculations for the $DO_{19}$ and $DO_{24}$ structures of $Ti_3Al$ using the FP-LMTO method. To see what structure is more stable one needs to compare the free energies of the two systems

$$G^i(x,p,V,T)=H^i(x,p,V)-TS^i(x)+F^i_{lv}(x,V,T), \quad (1)$$

where $H^i=E^i+pV$ is the enthalpy at temperature $T=0$ calculated from the energy per atom $E^i$ in a particular structure $i$ with a composition $x$ at volume $V$ and pressure $p$. The last two terms, the entropy $S^i$ and the free energy of the lattice vibrations $F_{lv}$, can be neglected at $T=0$. Calculated enthalpy difference between the $DO_{24}$ and $DO_{19}$ structures is shown in Fig. 1(b) by the solid line. The positive value in the complete pressure interval confirms our experimental observation that there is no pressure induced structural transition from $DO_{19}$ to $DO_{24}$ in $Ti_3Al$ up to 25 GPa, in contrast with what has been reported in Refs. 3,4. Notice that the energy difference between these two structures is very small indeed ($\sim$0.01 eV) in the whole pressure interval. Therefore, clearly there is a necessity for using the most accurate first-principles techniques, such as the FP method, in order to resolve it.

Several reasons for the disagreement between our present study and the one of Sahu *et al.*[3] can be identified. Different nature of the samples may be a possible reason for the discrepancy. The samples in both investigations were synthesized by arc melting. This technique itself cannot guarantee quality of a specimen, because of possible lose of material, oxidation, etc. Our samples were well characterized and the unit cell parameters were found to be in agreement with earlier studies and with theory (see Table I). The authors of Ref. 3 neither explained, why the unit cell parameters of their sample had discrepancies with those previously reported, nor analyzed probable reasons for internal inconsistency in their values of $a$ and $c$. According to Ref. 20, there is a well-established correlation between the unit cell dimensions and the Al content in $Ti_3Al$. The alloy studied in Ref. 3 had to

contain 19–22 at. % Al, according to the length of the *a* axis, but could not contain more than 15 at. % Al as judged from the *c* axis. The latter case corresponds to the two phase area (with $\alpha$-Ti) in the Al-Ti phase diagram. There are two more problems associated with presentation and interpretation of experimental data in Ref. 3. First, the diffraction patterns published in this paper do not contain any silver reflections, although Ag was used as a standard for pressure calibration. Second, the observed and calculated intensities of the diffraction peaks of the $DO_{24}$ structure at 16 GPa do not agree. Of course, the intensity mismatch in high-pressure x-ray diffraction experiments is a well known problem attributed to preferred orientation of particles in a diamond anvil cell. However, in such cases there should be a regularity in decrease or increase of intensities in certain directions. Such regularity is absent in data provided in Ref. 3.

The (101), (110), and (211) superlattice reflections and the (002) reflection of $Ti_3Al$ disappear at elevated pressures. The (101) and (110) reflections, $d \sim 3.88$ and 2.88 Å at ambient conditions, correspondingly, represent superlattice reflections with respect to the pure hcp structure of $\alpha$-Ti. The (110) reflection is difficult to observe using in-house x-ray facilities even in the initial diffraction pattern because of its low intensity (2 % in relative intensities). In all experiments, the (101) and (211) superlattice, as well as (002) and (202) reflections disappeared. To investigate whether it was a result of a preferred orientation or structural changes, the samples were extracted out of the gasket after the high-pressure experiments, and x-ray rotation scans were run at ambient conditions. The size of the samples was of 75 $\mu$m in diameter and a few $\mu$m thickness. In the diffraction patterns recorded at rotation, the (002) reflection was found [Fig. 2 curve (f)], i.e., their disappearance in high pressure experiments was a result of a strong preferred orientation developed on compression. At the same time, the (101) and (211) superlattice reflections were not found in any diffractogram. This means that their disappearance was not likely related to a preferred orientation. One plausible way to interpret this result would be to view it as a pressure-induced order-disorder phase transition on compression. However, our total energy calculations show that the enthalpy difference (at $T=0$) between the ordered $DO_{19}$ and the random hcp $Ti_{75}Al_{25}$ phase [dashed line in Fig. 1(b)] in fact increases as a function of pressure up to 25 GPa. Thus, the nature of this experimental effect needs to be studied by the use of more powerful x-ray sources.

In summary, we have investigated the behavior of $Ti_3Al$ with various Al content at pressures up to 25 GPa by means of *in situ* x-ray diffraction experiments and first-principles total energy calculations. The isothermal bulk moduli were obtained for three $Ti_3Al$ alloys from direct measurements of a unit cell volume as function of pressure, as well as from first-principles calculations. It was found, that the alloys with higher Al content are characterized by lower bulk moduli. For all three compositions of the $Ti_3Al$ alloys studied, no sign of the phase transition from the $DO_{19}$ to $DO_{24}$ structure was found. Thus the recent observation[3] of this phase transition was not confirmed. The only changes in the diffraction patterns on compression are the disappearance of some superlattice reflections in $Ti_3Al$ at pressures above 20 GPa.

This research was possible due to an equipment grant from the Wallenberg Foundation. This work has been partly supported by the Swedish Research Council for Engineering Sciences (TFR) and Natural Science Research Council (NFR). The support by the Swedish Materials Consortium No. 9 is acknowledged. I.A.A. is grateful to the Swedish Foundation for Strategic Research for financial support.

[1] W. D. Callister, Jr., *Materials Science and Engineering: An Introduction* (Wiley, Weinheim, 1996).

[2] *Alloys: Preparation, Properties, Applications*, edited by F. Habashi (Wiley, Weinheim, 1998).

[3] P. Ch. Sahu, N. V. Chandra Shekar, M. Yousuf, and K. Govinda Rajan, Phys. Rev. Lett. **78**, 1054 (1997).

[4] M. Rajagopalan, P. Ch. Sahu, N. V. Chandra Shekar, M. Yousuf, and K. Govinda Rajan, Int. J. Mod. Phys. B **13**, 841 (1999).

[5] L. S. Dubrovinsky, S. K. Saxena, P. Lazor, R. Ahuja, O. Eriksson, J. M. Wills, and B. Johansson, Nature (London) **388**, 362 (1997); L. S. Dubrovinsky, S. K. Saxena, F. Tutti, S. Rekhi, and T. LeBihan, Phys. Rev. Lett. **84**, 1720 (2000).

[6] *Mineral Physics and Crystallography: A Handbook of Physical Constants*, edited by J. Ahrens (AGU Reference Shelf, Washington, 1995).

[7] A MEW mixture in the ratio 16:3:1 was taken as a pressure-transmitting medium which provides hydrostatic environment up to 10–15 GPa. We obtain *in situ* high pressure powder x-ray diffraction data with a Siemens x-ray system consisting of a Smart CCD Area Detector and a direct-drive rotating anode as an x-ray generator (Mo$K_\alpha$ radiation-tube voltage 50 kV, tube current 24 mA, cathode gun 0.1×1 mm). With the capillary optic (x-ray optical stage, model CS-SRA/P-HP) installed, a high-intensity focus of x rays is produced at the sample position, and its width is controlled by a choice of a field aperture. A typical beam size in our experiments is about 80 $\mu$m in diameter. A long sample-detector distance (310 mm) allows us to derive very accurate data. Collecting time for each spectrum is up to 3 hours. At ambient conditions, x-ray powder diffraction data from the synthesized samples was collected on a Philips powder diffractometer (Cu-$K_\alpha$ radiation, tube voltage 40 kV, tube current 30 mA). Silicon was chosen as an internal standard. At the European Synchrotron Radiation Facilities data was collected at SNBL using monochromatic radiation of 0.7 Å wavelength and MAR 345 area detector. The beam size was 60 $\mu$m. The GSAS program was used to process diffraction data and calculate unit cell parameters with an accuracy better than $10^{-3}$ Å, A. Larson and R. Von Dreele, GSAS (General Structure Analysis System), LANSCE, MS-H805 (Los Alamos National Laboratory, Los Alamos, NM, 1994).

[8] E. Eremets, *High Pressure Experimental Methods* (Oxford University Press, Oxford, 1996).

[9] A. K. Singh, C. Balasingh, H. K. Mao, R. J. Hemley, and J. Shu, J. Appl. Phys. **83**, 7567 (1998).
[10] J. P. Perdew, K. Burke, and M. Ernzerhof, Phys. Rev. Lett. **77**, 3865 (1996).
[11] O. K. Andersen, Phys. Rev. B **12**, 3060 (1975); O. K. Andersen and O. Jepsen, Phys. Rev. Lett. **53**, 2571 (1984).
[12] J. M. Wills and B. R. Cooper, Phys. Rev. B **36**, 3809 (1987).
[13] I. A. Abrikosov and H. L. Skriver, Phys. Rev. B **47**, 16 532 (1993); A. V. Ruban, A. I. Abrikosov, and H. L. Skriver, *ibid.* **51**, 12 958 (1995).
[14] B. Johansson, R. Ahuja, O. Eriksson, and J. M. Wills, Phys. Rev. Lett. **75**, 280 (1995); R. Ahuja, O. Eriksson, J. M. Wills, and B. Johansson, *ibid.* **75**, 3473 (1995); S. I. Simak, U. Häussermann, I. A. Abrikosov, O. Eriksson, J. M. Wills, S. Lidin, and B. Johansson, *ibid.* **79**, 1333 (1997).
[15] J. Trygg, B. Johansson, O. Eriksson, and J. M. Wills, Phys. Rev. Lett. **75**, 2871 (1995).
[16] E. Enc and B. Margolin, J. Met. **9**, 484 (1957).
[17] B. Goldak and B. Parr, Trans. Am. Inst. Min., Metall. Pet. Eng. **221**, 639 (1961).
[18] A. Penalosa and C. R. Houska (unpublished).
[19] O. L. Anderson, *Equation of State of Solids for Geophysics and Ceramic Science* (Oxford University Press, Oxford, 1995).
[20] J. L. Murray, in *Binary Alloy Phase Diagrams*, edited by T. B. Massalski *et al.* (ASM International, New York, 1990), p. 173.